In-Situ Neutron Scattering Measurement of Stress-Strain Behavior of a Bulk Metallic Glass

TIMOTHY WILSON, BJØRN CLAUSEN, THOMAS PROFFEN, JENNIFER ELLE, and DON BROWN

Bulk metallic glasses (BMGs) are an emerging class of materials whose unique properties make them excellent choices for many applications. As with crystalline metals, the processing and forming techniques used to produce BMG components necessarily result in residual stresses. However, traditional diffraction stress analysis is difficult to apply to BMG components, because they lack the long-range order necessary to produce sharp diffraction patterns, and thus, the internal strains for BMG have not been examined until recently. In this work, *in-situ* neutron scattering was used to measure the local elastic internal strain distribution in a $Zr_{57}Nb_5Cu_{15.4}Ni_{12.6}Al_{10}$ BMG as a function of applied stress. Various techniques were used to evaluate the internal strain. The strain was determined in real space, by measuring changes in the atomic pair distribution function (PDF). These results can be used to help understand the elastic deformation of BMGs as well be to evaluate current models of BMG deformation.

DOI: 10.1007/s11661-007-9268-5

I. INTRODUCTION

METALLIC glasses are an important new class of engineering materials with attractive properties such as high strength, high hardness, a large elastic strain limit (~2 pct), and good fracture toughness.[1–4] Because of their amorphous structure and inherent lack of grains, metallic glasses do not deform due to dislocation motion as do most crystalline materials. At room temperature, they generally deform *via* localized shear bands, which quickly propagate through the materials, quickly leading to catastrophic failure.[5] Because metallic glasses form these localized shear bands, typically leading to failure before appreciable plastic deformation can occur, understanding the internal strains during elastic deformation is an important aspect of understanding the deformation in these materials. Modeling of the deformation of bulk metallic glasses (BMGs) began about 35 years ago,[6–8] but these models have not been verified by experiments because experimental techniques for measuring the internal stress-strain behavior of glasses were not available. Today high-intensity synchrotron X-ray and pulsed neutron diffraction facilities make *in-situ* loading diffraction experiments possible. An understanding of the deformation behavior at all length scales (*i.e.*, nanoscale, microscopic, and macroscopic) is still required for these materials, and considerable effort is being put forth to understand the deformation and fracture of metallic glasses.[9–12] Because most of the deformation at room temperature is elastic, and because of the high elastic deformation limit of BMGs, they should be a good candidate for strain measurements *via* diffraction. The primary challenge to studying the deformation of metallic glasses by diffraction is that metallic glasses are not crystalline. They do not produce sharp crystalline peaks, whose changes can be easily and accurately measured. The diffraction pattern of metallic glasses consists of a broad hump, which has typically been considered useless for accurate strain measurements.

X-ray and neutron diffraction have been used to measure elastic strains in crystalline engineering materials for a long time. This is done by measuring changes in the *d*-spacing of atomic planes, and the microscopic diffraction data can be accurately correlated to macroscopic properties. Recently, efforts have been made to use high-energy X-rays as a tool to measure elastic strains in amorphous materials.[13,14] Because high-energy X-rays and neutrons can be used to examine the local atomic structure of materials, these techniques have been employed to examine structural changes of glasses that have been subjected to large stresses. This report presents recent efforts to examine the deformation of $Zr_{57}Nb_5Cu_{15.4}Ni_{12.6}Al_{10}$ by using neutron diffraction.

II. EXPERIMENTAL

Ingots of the $Zr_{57}Nb_5Cu_{15.4}Ni_{12.6}Al_{10}$ alloy were prepared by arc melting elemental metals with purity

TIMOTHY WILSON, Graduate Student, is with the Department of Materials Science and Engineering, University of Tennessee, Knoxville, TN 37996, USA. Contact e-mail: twilson3@utk.edu BJØRN CLAUSEN, SMARTS Instrument Scientist, and THOMAS PROFFEN, NPDF Instrument Scientist, are with the Lujan Neutron Science Center, Los Alamos National Laboratory, Los Alamos, NM 87545, USA. JENNIFER ELLE, Undergraduate Student, is with the Department of Physics, University of Idaho, Moscow, ID 83843, Russia. DON BROWN, SMARTS Instrument Scientist, is with the Materials Science and Technology Division, Los Alamos National Laboratory, Los Alamos, USA.

This article is based on a presentation given in the symposium entitled "Bulk Metallic Glasses IV," which occurred February 25–March 1, 2007 during the TMS Annual Meeting in Orlando, Florida under the auspices of the TMS/ASM Mechanical Behavior of Materials Committee.

Article published online August 4, 2007

of 99.7 pct or higher in a Ti-gettered Ar atmosphere, which was evacuated to about 3×10^{-2} Torr and flushed with Ar gas several times. While still under vacuum, it was heated to 975 °C and held there for 10 minutes to melt the $Zr_{57}Nb_5Cu_{15.4}Ni_{12.6}Al_{10}$ alloy. After melting the metallic glass, the temperature was lowered to 875 °C and held for another 15 minutes during which 100 psi Ar gas pressure was applied to force the molten alloy into the tube. This was followed by quenching the tube in water at room temperature. Test samples were machined into a cylindrical geometry of 6-mm diameter and 14.4-mm length.

Neutron diffraction experiments were conducted under uniaxial compression on the spectrometer for materials research at temperature and stress (SMARTS) instrument at the Lujan Neutron Science Center, Los Alamos National Laboratory. The geometric setup of SMARTS allows for simultaneous measurements in longitudinal and transverse directions. The diffraction data were collected using the time-of-flight technique for 4 hours at each stress level, ranging from 20 to 1500 MPa, and after unloading to 20 MPa. Data were collected to a maximum q of 20.4 Å^{-1}.

III. RESULTS

Measurements were performed such that the BMG sample was initially loaded to a stress of 20 MPa in order to hold the sample in the horizontal load frame. The sample was held at this stress while the diffraction measurement was conducted. After sufficient data were collected, the stress was increased to 500 MPa and this procedure was repeated. Data were collected at stresses of 20, 500, 1000, 1500 MPa, and after unloading the sample back to 20 MPa. The macroscopic stress-strain behavior was measured in compression with an affixed extensometer for applied stresses ranging from 0 to 1500 MPa. The macroscopic data show that the deformation in the BMG is fully reversible, because the loading and unloading portions of the stress-strain curve were directly on top of each other. The elastic modulus measured from the slope of the stress-strain curve was 84 GPa.

The pair distribution functions (PDFs) possess useful local atomic pair information, such as the distances between central and neighboring atoms and the nature of neighboring atoms.[15] By measuring changes in the PDF under applied loads, it is possible to gain information about how the local atomic structure changes during deformation. The PDF, $G(r)$, was computed using the program PDFgetN[16] *via* the Fourier transform of $Q[S(Q) - 1]$:

$$G(r) = \frac{2}{\pi} \int_0^\infty Q[S(Q) - 1] \sin(Qr) dQ \qquad [1]$$

where $S(Q)$ is the structure factor and Q is the scattering vector ($Q = 4\pi \sin \theta/\lambda$).

Analysis of glasses using the PDF assumes that the BMGs are isotropic and amorphous materials are usually assumed to be isotropic. In this case, the assumption is made that the small amount of anisotropy causing the uniaxial deformation can be neglected even though a thorough analysis would involve using spherical harmonics to describe the small amount of anisotropy.[17,18] The PDFs, $G(r)$, shown in Figure 1(a), for the axial direction have been obtained through the Fourier transformation of the structure factor, $S(q)$, data. The first coordination shell of $G(r)$ shows that the peak shifts to smaller r with increasing compressive load, indicating that the atom-atom pair distances are being shortened or compressed (Figure 1(b)). When the sample was unloaded from 1,500 to 20 MPa, all of the strain was recovered to a level very close to the initial loading condition of 20 MPa.

For each loading condition, strain was calculated by measuring the shift of each $G(r) = 0$ intercept relative to the initial loading condition for distances up to $r = 16$ Å. The strains determined from $G(r)$ from the

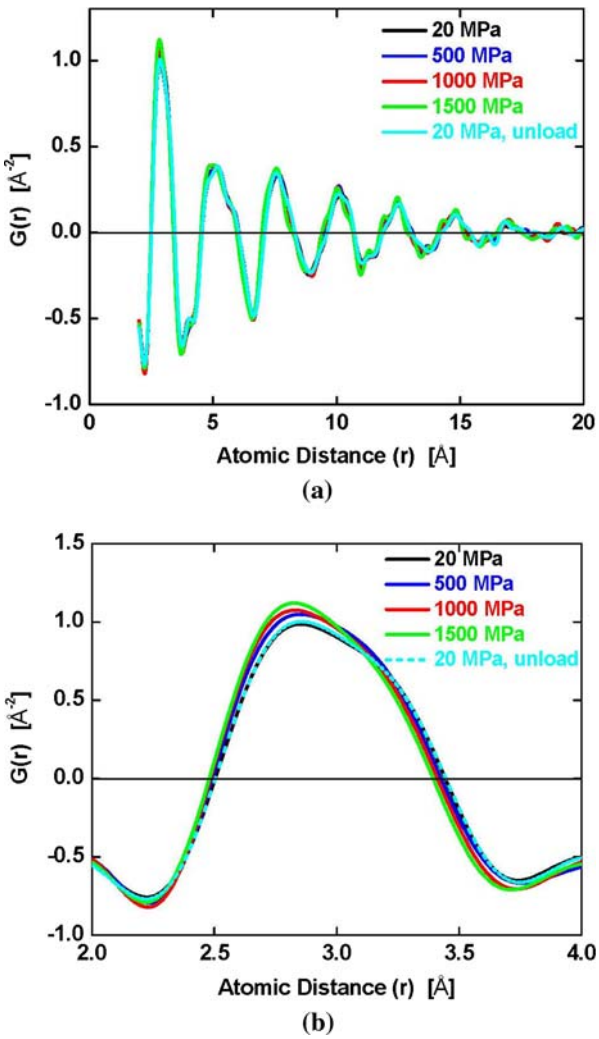

Fig. 1—(*a*) PDF $G(r)$ calculated from the $S(q)$ diffraction data measured on $Zr_{57}Nb_5Cu_{15.4}Ni_{12.6}Al_{10}$ using SMARTS instrument. (*b*) First correlation shell of the PDF measured $Zr_{57}Nb_5Cu_{15.4}Ni_{12.6}Al_{10}$ using SMARTS instrument, showing shift of PDF toward compressive strains as load is applied.

axial bank of the SMARTS instrument are plotted as a function of distance r out to ~16 Å for the different stress levels in Figure 2. Distances greater than 16 Å in the PDF (Figure 1(a)) approach zero indicating that there is no order past 16 Å. There appears to be no significant trend for increasing strain as the distance in the PDF increases. This is significantly different than was reported by Paulsen,[13] in which it was reported that strain increased by a factor of 2.7 beyond the first coordination shell. The data show that at a distance of about 9 to 10 Å and 15 to 16 Å, there are spikes in the strain data that are seen for each level of applied stress. Similar spikes in strain were reported on a similar metallic glass (Vit105–$Zr_{57}Ti_5Cu_{20}Ni_8Al_{10}$) at distances of 8 to 9 Å and 13 to 15 Å.

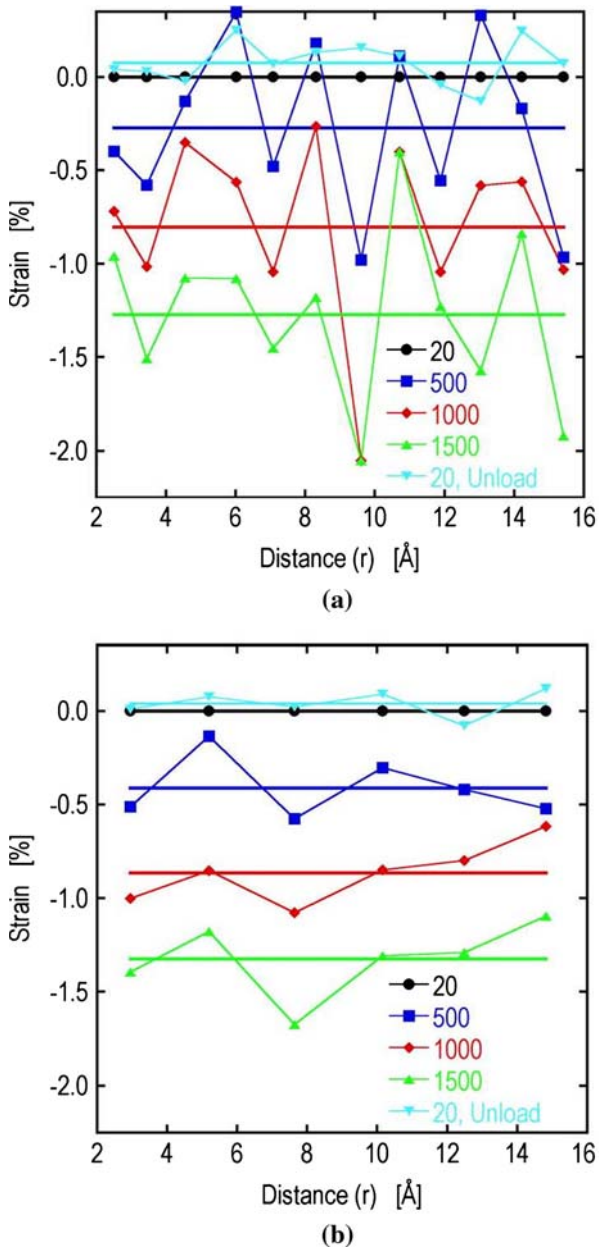

Fig. 2—(*a*) Intercept strain data calculated from $G(r)$ as a function distance r for $Zr_{57}Nb_5Cu_{15.4}Ni_{12.6}Al_{10}$. (*b*) Center-of-mass strain as a function of distance determined from PDF analysis for $Zr_{57}Nb_5Cu_{15.4}Ni_{12.6}Al_{10}$.

The average strain was determined by taking an average of all strains for each stress over the complete range of r measured. This linear fit yields an elastic modulus value E = 121 GPa (Figure 3). The elastic modulus of $Zr_{57}Nb_5Cu_{15.4}Ni_{12.6}Al_{10}$ reported in the literature is 87.3 GPa,[19] a 39 pct difference. By calculating the slope from the transverse direction data, the Poisson's ratio, ν, was calculated to be 0.52. The literature value for ν = 0.365, a difference of ~42 pct.

Statistical methods were also used to measure the local deformation of the BMG. The center of mass of each peak in the PDF was calculated according to the equation

$$COM = \frac{\oint rG(r)dr}{\oint G(r)dr} \qquad [2]$$

Strain was calculated by measuring the change in the center of mass of each coordination shell as a function of stress. This gives an average of how the bulk of the atoms in each coordination shell is moving with stress. It is less sensitive to the termination ripples of the PDF data, which could affect the stress strain behavior calculated using the intercept method. This is because it is a weighted average and is less responsive to the data farther from the center of the mass of each coordination shell. The center of mass data was plotted to give strain as a function of distance r (Figure 2(b)). The data show that as stress is applied, the strain increases in a very similar manner observed in the intercept method. When the stress is lowered back to 20 MPa, the strain decreases to a level near the initial condition of 20 MPa, as expected for a fully recoverable deformation process. The average strain from all of the coordination shells results in an obtained modulus value of about 112 GPa, which is within the error bars calculated for the intercept method, as seen in Figure 3. The difference between the literature data and the center-of-mass determination of Young's modulus and Poisson's ratio is 29 and 32 pct, respectively.

IV. DISCUSSION

It was noted previously that the first coordination shell of BMGs is stiffer than the bulk average of the material taken at a large value of r. This appears to be the case for the $Zr_{57}Nb_5Cu_{15.4}Ni_{12.6}Al_{10}$ alloy as well. The elastic modulus of the first $G(r)$ = 0 intercept (corresponding to the first coordination shell) was measured to be 145 GPa, while the second intercept and the bulk (everything outside of the first shell) give values of 97 and 107 GPa, respectively. The values of the elastic moduli in the glass in the first shell likely are due to overlapping Zr-(Cu, Ni) and (Cu, Ni)-(Cu, Ni) bonds and Zr – Zr bonds, as these values are similar to the crystalline materials. The left side of the first coordination shell had a stiffness of 145 GPa, while the right side had a stiffness of 97 GPa. The elastic

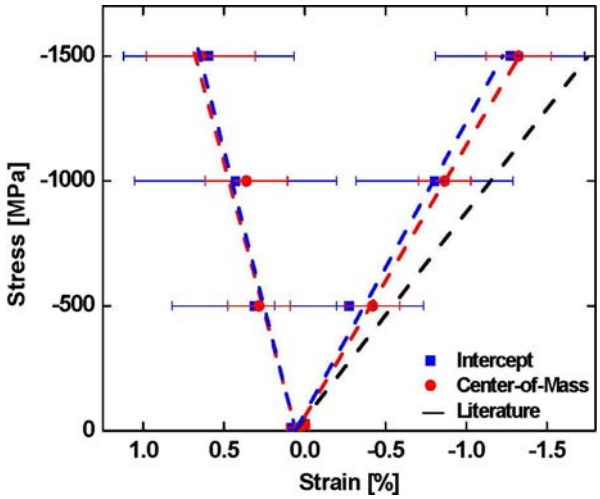

Fig. 3—Stress *vs* strain curve for $Zr_{57}Nb_5Cu_{15.4}Ni_{12.6}Al_{10}$ calculated on SMARTS from average local strains in $G(r)$ by the intercept method and the center of mass method.

modulus of crystalline Zr is 96 GPa, Cu is 115 GPa, and Ni is 204 GPa.[20] Based on atomic size calculations, the left side of the first coordination shell is primarily Zr-Zr bonds, while the right side is dominated by Zr-(Ni, Cu) and (Ni, Cu)-(Ni, Cu) bonds. The presence of Al and Nb, in the diffraction data, is difficult to observe in the diffraction data due to the low scattering cross section of Al and the low concentration of Nb in the alloy. This could be important when comparing the diffraction data to the macroscopic data, because at 10 and 5 pct, the concentration of these elements is likely higher than can be neglected on the macroscopic scale.

The difference between the measured local elastic modulus of ~112 GPa and the literature value of ~87 GPa is about 29 pct. This difference is about the same as the difference between glasses and their corresponding crystalline counterparts.[21,22] This difference in modulus is likely due to internal displacements or rearrangements, which can occur in glasses but cannot in crystals.[6,7] In crystals, atoms are located at the centers of symmetry, and the atomic displacements are completely described by the macroscopic displacement field. Glasses can have additional displacement options due to the regions of lower density caused by their amorphous nature, and some atoms will be strained more than others. The free volume present in metallic glasses allows atoms to move in a uniform direction with the applied stress and in a nonuniform direction with applied stress, and thus anelastic deformation can occur in glasses in addition to elastic deformation. These inhomogeneous displacements cause decreases in the shear modulus and Young's modulus in glasses.[23] The diffraction results would show the component of the strain in which the atoms moved in the same direction. The additional motion component of the strain in which the atoms are displaced in different directions would not appear in the analysis of the diffraction data. This effect can be removed to some degree by structurally relaxing the glass, such as by annealing the glass below T_x. The slight densification associated with structural relaxation has been shown to substantially raise the Young's modulus closer to that of the devitrified state.[24]

If atoms in metallic glasses have short-range order, and solute atoms tend to cluster around solvent atoms,[25–27] this effect would be seen by the movement of clusters as opposed to individual atoms. The shear displacement of clusters would not be observed in the local structure because average local environment would be the same. In this way, the atoms could move in a uniform manner under the applied stress that would be measured by diffraction, and at the same time the clusters themselves could rotate and arrange themselves in a way to minimize internal energy.[28] Rotation would be allowed by the additional volume frozen into the glass, and a collective rotation of clusters could serve to initiate shear bands, which appear at higher stresses near the yield stress. The space between clusters, acting as free volume, would provide room for the rotation of clusters upon applied loading, helping to govern the deformation characteristics of the glass.[29]

In order to investigate this phenomenon, the changes in the peak width were examined by studying the variance of each coordination shell in the PDF. The normalized change in the variance, $(\sigma^2 - \sigma^2_o)/\sigma^2_o$, where σ^2 is the variance of the coordination shell and σ^2_o is the variance of the coordination shell in the initial loading condition, was calculated for each loading condition as a function of distance r. These data are plotted in Figure 4. While the center of mass measurements shows how the weighted center of the peaks moves as a stress is applied, the variance of the data, which is a measure of how the data are distributed about the center of mass, illustrates how the extremes of the data change with regard to the center of mass. Figure 4 indicates that in the fourth shell, r ~ 10 Å, the extremes move significantly more than the center of mass for each applied load. After this spike in the data, the variance appears to move in the negative direction to a spike at around 15 Å. These spikes are due to the coordination shell broadening and contracting at different distances as the stress is applied. This means that the environment at

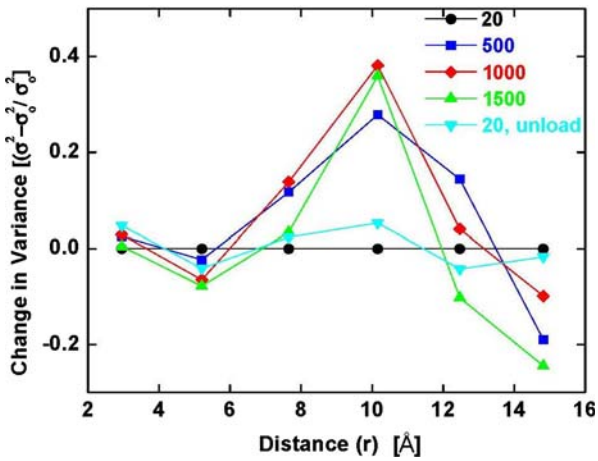

Fig. 4—Change in variance from the center of mass measurements as a function of distance r measured on $Zr_{57}Nb_5Cu_{15.4}Ni_{12.6}Al_{10}$ BMG.

distances of about 10 Å from an average atom is being deformed more than atoms at smaller average distances. These spikes are present at all levels of stress, and the unloaded sample shows that this deformation in the broadening and contracting of the coordination shells is recoverable.

While the average local strain is less than the macroscopic response, there are instances where the local strain exceeds the macroscopic behavior. While looking at the data obtained from the intercept method, this happens at distances of 9 to 10 Å and 15 to 16 Å. A similar spike in the data was observed at ~10 Å when the variance from the center of mass was plotted as a function of distance, and this spike disappears upon unloading. Interestingly, these spikes in strain correspond nicely to the diameter expected for shear transformation zones (STZs), ~10 Å, or roughly 3 or 4 atoms in diameter.[30–32] The 3 or 4 atoms in diameter could then correspond to the size of one local cluster of atoms arranged with short-range-ordering schemes. The STZ is a deformation mechanism caused by the collective motion of atoms (possibly the atoms within a cluster rotating together) subjected to shearing forces. Multiple STZs acting together can be thought of as a shear band nucleus. The STZ is a way for local shear events to comprise local plasticity. These local plastic strains could explain why the average strain measured is less than the macroscopic response of the material, because plastic deformation would not be detected *via* diffraction measurements. Local plastic deformation through the rotation of clusters could explain the anelastic deformation behavior observed in this experiment along with the spikes in the strain data occurring at distances of about 10 Å.

V. CONCLUSIONS

The internal strain was measured for a $Zr_{57}Nb_5Cu_{15.4}Ni_{12.6}Al_{10}$ BMG *in situ* by neutron diffraction. Measurements of the stress-strain behavior were examined by multiple data analysis methods in real space with good precision. The results show that local strains can be measured, and the deformation of metallic glasses appears to be due to elastic dilatations along with localized plastic deformation of clusters of atoms that occur in glasses but not in crystals. These results seem to validate the idea that metallic glasses contain short-range order, and metallic glass deformation occurs at multiple length scales.

ACKNOWLEDGMENTS

This work has benefited from the use of the Los Alamos Neutron Science Center at the Los Alamos National Laboratory. This facility is funded by the United States Department of Energy under Contract No. W-7405-ENG-36.

REFERENCES

1. A. Inoue: *Bulk Amorphous Alloys: Preparation and Functional Characteristics*, Trans Tech Publications, Uetikon-Zuerich, Switzerland, 1989, pp. 1–15.
2. W.L. Johnson: *Intermetallic Compounds*, Vol. 1, Wiley, New York, NY, 1994, p. 687.
3. W.L. Johnson: *JOM-J. Miner. Met. Mater. Soc.*, 2002, vol. 54, pp. 40–43.
4. C.J. Gilbert, R.O. Ritchie, and W.L. Johnson: *Appl. Phys. Lett.*, 1997, vol. 71, pp. 476–78.
5. B. Yang, P.K. Liaw, G. Wang, M. Morrison, C.T. Liu, R.A. Buchanan, and Y. Yokoyama: *Intermetallics*, 2004, vol. 12, pp. 1265–74.
6. D. Weaire, M.F. Ashby, J. Logan, and M.J. Weins: *Acta Metall.*, 1971, vol. 19, pp. 779–88.
7. G. Knuyt, L. Deschepper, and L.M. Stals: *J. Phys. F Met. Phys.*, 1986, vol. 16, pp. 1989–2006.
8. A.S. Argon and L.T. Shi: *Acta Metall.*, 1983, vol. 31, pp. 499–507.
9. H.A. Bruck, T. Christman, A.J. Rosakis, and W.L. Johnson: *Scripta Metall. Mater.*, 1994, vol. 30, pp. 429–34.
10. R.A. Connner, A.J. Rosakis, W.L. Johnson, and D.M. Owen: *Scripta Mater.*, 1997, vol. 37, pp. 1373–78.
11. C.T. Liu, L. Heatherly, D.S. Easton, C.A. Carmichael, J.H. Schneibel, C.H. Chen, J.L Wright, M.H. Yoo, J.A. Horton, and A. Inoue: *Metall. Mater. Trans. A*, 1998, vol. 29A, pp. 1811–20.
12. T.C. Hufnagel, C. Fan, R.C. Ott, J. Li, and S. Brennan: *Intermetallics*, 2002, vol. 10, pp. 1163–66.
13. H.F. Poulsen, J.A. Wert, J. Neuefeind, V. Honkimaki, and M. Daymond: *Nature Mater.*, 2005, vol. 4, pp. 33–36.
14. T.C. Hufnagel, R.T. Ott, and J. Almer: *Phys. Rev. B*, 2006, vol. 73, p. 064204.
15. T. Proffen, S.J.L. Billinge, T. Egami, and D. Louca: *Z. Kristallogr.*, 2003, vol. 218, pp. 132–43.
16. P.F. Peterson, M. Gutmann, T. Proffen, and S.J.L. Billinge: *J. Appl. Crystallogr.*, 2000, vol. 33, p. 1192.
17. M.E. Milberg: *J. Appl. Phys.*, 1962, vol. 33, pp. 1766–68.
18. Y. Suzuki, J. Haimovich, and T. Egami: *Phys. Rev. B*, 1987, vol. 35, pp. 2162–68.
19. J. Lewandowski, W. Wang, and A.L. Greer: *Phil. Mag. Lett.*, 2005, vol. 85, pp. 77–87.
20. G. Simmons and H. Wang: *Single Crystal Elastic Constants and Calculated Aggregate Properties: A Handbook*, 2nd ed., MIT Press, Cambridge, MA, 1971.
21. M.F. Ashby, A.N. Nelson, and R.M. Centamor: *Scripta Metall.*, 1970, vol. 4, pp. 715–17.
22. M. Barmatz and H.S. Chen: *Phys. Rev. B*, 1974, vol. 9, pp. 4073–83.
23. D. Srolovitz, V. Vitek, and T. Egami: *Acta Metall.*, 1983, vol. 32, pp. 335–52.
24. H.S. Chen: *J. Appl. Phys.*, 1978, vol. 49, pp. 3289–91.
25. D. Miracle, W. Sanders, and O. Senkov: *Phil. Mag. A*, 2003, vol. 83, pp. 2409–28.
26. D. Miracle: *Nat. Mater.*, 2004, vol. 3, pp. 697–702.
27. H.W. Sheng, W.K. Luo, F.M. Alamgir, J.M. Bai, and E. Ma: *Nature*, 2006, vol. 439, pp. 419–25.
28. C. Fan, P.K. Liaw, T.W. Wilson, W. Dmowski, H. Choo, C.T. Liu, J.W. Richardson, and T. Proffen: *Appl. Phys. Lett.*, 2006, vol. 89, p. 111905.
29. C. Fan, P.K. Liaw, V. Haas, J.J. Wall, H. Choo, A. Inoue, and C.T. Liu: *Phys. Rev. B*, 2006, vol. 74, p. 014205.
30. A.S. Argon: *Acta Metall.*, 1979, vol. 27, pp. 47–58.
31. A.S. Argon and L.T. Shi: *Acta Metall.*, 1983, vol. 31, pp. 499–507.
32. C.A. Schuh, A.C. Lund, and T.G. Nieh: *Acta Mater.*, 2004, vol. 52, pp. 5879–91.